Thermal buckling of coated functionally graded plates under non-uniform temperature rises

EL IBRAHIMI MOHAMED[1*], ABDERRAHIM SAMAOUALI, LAHCEN AZRAR[2], ABDERRAHIM DINANE[3], ABDELLATIF RAHMOUNI[4]

[1]Team Thermodynamic Energy Faculty of Sciences, Energy center, Mohammed V University, B.P. 1014, Rabat, Morocco B.P.1014, 10090, Rabat, MOROCCO
[2]Research center STIS, M2CS, Department of Applied Mathematics and Informatics, ENSET, UM5, Rabat, MOROCCO
[3] Département de Recherches et Projets, Laboratoire de Thermodynamique, Ecole Royale Navale Boulevard Sour Jdid, Casablanca 20000, MAROCCO
[4]Laboratoire de Mécanique, Productique et Génie Industriel, Ecole Supérieure de Technologie de Casablanca Université Hassan II de Casablanca, MAROCCO
*mohamed.elibrahimi@um5s.net.ma

Abstract: Recently, the functionally graded (FG) concept used in different mechanical engineering applications has become an important solution for delamination problems due to the brutal transition of material composition. The specific goal of this study is the determination of theoretical solution of the critical buckling temperature for rectangular FG plates with a ceramic coating, subjected to the sinusoidal and power law temperature rises. By applying the Galerkin method, the critical buckling load model is obtained. Based on obtained results, the effect of coated functionally graded parameters, namely the coating thickness, the power law index, the initial imperfections and the temperature rise type on the thermal buckling is discussed. This study is useful for the design engineers to choose the coating thickness, the geometrical parameters and the optimum composition as desired to assure the stability of structures subjected to a non-uniform temperature distribution.

Key-words: Functionally graded plate, Ceramic coating, Thermal buckling, Classical plate theory.

1 Introduction

The functionally graded materials (FGMs) where developed to be able to withstand a surface temperature of 2100 K and a temperature gradient of 1600 K across a thickness less than 10 mm [1]. Different from classical composite materials, FGMs has a gradual change from one material to the other. This concept was used as thermal barriers in fusion reactors and aerospace structural applications, and later in structural parts at very high operation temperatures. In the field of aeronautics and marine, coated FGM plates have shown their reliability, in terms of thermal insulation and corrosion resistance more than metal material in high temperature environment. So, when FGMs are exposed to high temperature fields, their structural integrity will be lost and becomes geometrically unstable and it is essential to consider this problem in the design process of these structures. More researchers show a vital role in mathematical modeling to predicting the accurate behavior of the coated or sandwich FGM plate and shell.

Based on the classical plate theory, Javaheri and Eslami [2] derived the expression of the critical temperature difference corresponding to the buckling of geometrically perfect FGM plates, Kiani Y.and al. [3] studied the thermal buckling of rectangular plates resting on elastic foundations and several types of thermal loading were considered in their works. Lanhe W.[4] used the classical plate (CPT) and first order shear deformation (FSDT) theories to study the thermal buckling of FGM plates. Shariat and Eslami [5–7] presented the thermal buckling analysis of functional gradient rectangular plates with geometric imperfections using the classical plate theory (CPT). The work was extended to study the same problematic by using the first order shear deformation (FSDT) and the third order shear deformation (TSDT) theories. Three types of temperature field across the thickness are studied. Investigations in the effect of geometrical imperfections on buckling and post buckling behaviors by using high order shear deformation theory (HSDT) are been carried out by

Yang and al. [8]. Tung and Duc [9] studied the buckling response of FGM plates with geometric imperfections based on CPT. Fiorenzo A. and Fazzolari [10] used the advanced hierarchical trigonometric Ritz formulation (HTRF) to analyze the free vibration and thermal stability of FGM sandwich plates under the effect of uniform and non-uniform temperature rises. Reddy [11] analyzed the behavior of the rectangular FG plates based on the theory of the third order shear deformation plate. Shi-Rong and al. [12] used Shooting Method to study the nonlinear thermo-mechanical post buckling for an imperfect FGM circular plate, subjected to both mechanical load and transversely uniform and power law temperature rises. Zenkour and Sobhy [13] studied different types of symmetric FGM sandwich plates with sinusoidal shear deformation plate theory assuming the thermal loads uniform, linear and non-linear through-the-thickness. Hui-Shen [14] includes the temperature-dependence properties to study the thermal post buckling behavior of shear deformable FGM plates.
Recently, Galerkin method was successfully used by many researchers in the resolution of buckling problems with geometrical imperfections. Hoang [15,16] studied the post buckling behavior of FGM sandwich plates, and FGM shallow spherical shells resting on elastic fondations and subjected to uniform external pressure, thermal loading and uniaxial compression in thermal environment taking acount also the degree of tangential restraint. Zewu and al. [17] also employed the Galerkin method to study the buckling behavior of coated imperfect cylindrical shells. In their work, the problem was solved in the case of uniform and linear thermal loads. Sofiyev [18] proposed investigating the buckling of FGM conical shells, under uniform and linear temperature rises, by applying the shear deformation theory (SDT). Based on the same theory, Sofiyev and al. [19] continued the previous work by studying the case of a nonlinear thermal load.
The role of coating allows providing FG structures against failure mechanisms caused by molten salt such as corrosion and CMAS (CaO-MgO-Al2O3-SiO2) effect especially in aircraft and marine. The thermal buckling study of coated FG plates subjected to nonlinear temperature rise has not studied before. Therefore, the actual paper develops this problem. Two types of nonlinear temperature field are investigated such the power law and sinusoidal. The composition is supposed to be graded through the thickness direction. Governing equations are established taking into account geometrical imperfections and introducing Von Karman nonlinearity due to large deformations. The plates are assumed to be simply supported on edges that are radically immovable. Approximate solutions are assumed to satisfy boundary conditions and the Galerkin method is adopted to obtain explicit expressions of the buckling load and temperature-deflection relations. The pre-buckling critical buckling temperature diagrams were constructed and an analysis of the effect of coating-thickness ratio, the geometrical imperfection and the power law index on the thermal buckling behavior is carried out. The obtained results are validated with those of earlier work [9].

2 Fundamental equations of FGM plate with coating

2.1 Material properties

Based on the Cartesian coordinates (x, y, z), we consider an imperfect thin rectangular FGM plate with coating. In the Fig. 1, the parameters a, b and h represent the length, width and thickness of the plate respectively, and h_c is the ceramic coating thickness. The material components are changed from a metal surface $(z = -h/2)$ in the bottom face to a ceramic surface $(z = h/2 - h_c)$ in the intermediate face; meanwhile, a ceramic coating with a thickness h_c, was subsequently deposed on the FGM plate.

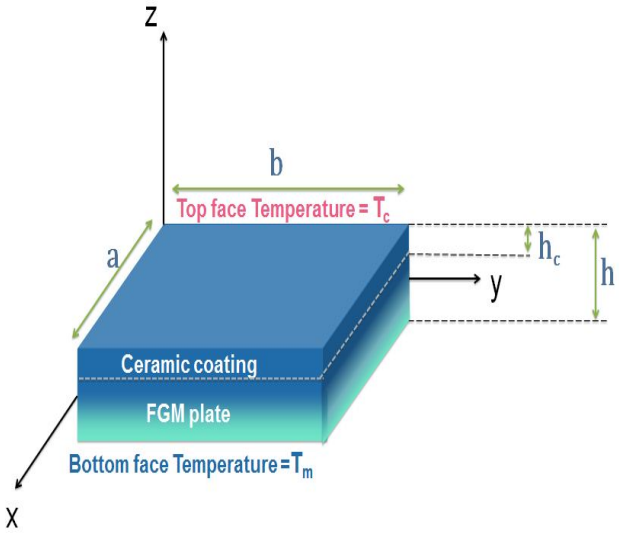

Fig. 1. Configuration and coordinate system for FGM plate with coating.

The material properties such as the Young's modulus, the thermal conductivity and the coefficient of thermal expansion, are defined by the law of mixture. The Poisson's ratio is considered to be constant through the thickness direction because the effect of this ratio on the buckling phenomenon is much less than others material properties [20].

The material property P is given by the following equation:

$$P(z) = P_m + (P_c - P_m)\, V(z) \quad (1)$$

where subscribes c and m indicate the ceramic and metal constituents respectively. $V(z)$ is the volume fraction of the ceramic phase and according to the power law, it is defined by:

$$V(z) = \begin{cases} \left(\frac{2z+h}{2(h-h_c)}\right)^k & ; \quad -\frac{h}{2} \le z \le \frac{h}{2} - h_c \\ 1 & ; \quad +\frac{h}{2} - h_c \le z \le \frac{h}{2} \end{cases} \quad (2)$$

where k is the volume fraction index($k > 0$), and also denotes the non-homogeneous parameter characterizing the degree of the material gradient in the z-direction.

2.2 Theoretical formulations

2.2.1 Kinematics

To establish the governing equations and determine the buckling loads of the imperfect FGM plates, the classical plate theory (CPT) is used.

The displacements of a generic material point, located at (x, y, z) in the plate, may be written as follows:

$$U(x,y,z) = u(x,y) - z\frac{\partial w}{\partial x} \quad (3)$$

$$V(x,y,z) = v(x,y) - z\frac{\partial w}{\partial y}\ , \quad (4)$$

$$W(x,y,z) = w(x,y) \quad (5)$$

where $u(x,y), v(x,y),$ and $w(x,y)$, denote displacement components of point on the mid-plane ($z = 0$) along the x, y and z directions respectively.

When the plate deflections are not small compared with the plate thickness, there is a coupling between the membrane and bending actions of the plate which evinces itself in two important respects. The strains in the plane of the plate are found to be dependent on non-linear terms in the deflection w; and the equation of equilibrium for forces in the z direction contains significant terms derived from the components of the force resultants N in the distorted median plane [21] (see the third term of Eqs. (24)). Therefore, the strains across the plate thickness at a distance z from the middle surface are [9,13,15]:

$$\varepsilon_x = \varepsilon_{x0} - z\,\frac{\partial^2 w}{\partial x^2} \quad (6)$$

$$\varepsilon_y = \varepsilon_{y0} - z\frac{\partial^2 w}{\partial y^2} \quad (7)$$

$$\gamma_{xy} = \gamma_{xy0} - 2z\frac{\partial^2 w}{\partial x\,\partial y} \quad (8)$$

where $\varepsilon_{x0}, \varepsilon_{y0},$ and γ_{xy0} represent the strains of point on the mid-plane (z=0) and are given by:

$$\varepsilon_{x0} = \frac{\partial u}{\partial x} + \frac{1}{2}\left(\frac{\partial w}{\partial x}\right)^2 \quad (9)$$

$$\varepsilon_{y0} = \frac{\partial v}{\partial y} + \frac{1}{2}\left(\frac{\partial w}{\partial y}\right)^2 \quad (10)$$

$$\gamma_{xy0} = \frac{\partial u}{\partial y} + \frac{\partial v}{\partial x} + \frac{\partial w}{\partial x}\frac{\partial w}{\partial y} \quad (11)$$

2.2.2 Constitutive relations and equilibrium equations

Assuming the material of the plate obeying Hooke's law, and by considering the thermal effects, the constitutive relations are given by:

$$\sigma_x = \frac{E(z)}{1-\nu^2}\left[\varepsilon_x + \nu\varepsilon_y - (1+\nu)\alpha T\right] \quad (12)$$

$$\sigma_y = \frac{E(z)}{1-\nu^2}\left[\varepsilon_y + \nu\varepsilon_x - (1+\nu)\alpha T\right] \quad (13)$$

where $\sigma_x,\ \sigma_y$ are the normal stresses. The shear τ_{xy} is given by:

$$\tau_{xy} = G(z)\,\gamma_{xy} \quad (14)$$

where the term G(z) is the shear modulus and related to young's modulus E(z) by:

$$G(z) = \frac{E(z)}{2(1+\nu\ )} \quad (14\text{ bis})$$

By using the constitutive equations, and the resultant forces and moments are found to be [9]:

$$(N_{ij}, M_{ij}) = \int_{-\frac{h}{2}}^{\frac{h}{2}} \sigma_{ij}\,(z, z^2)dz \quad ;$$

$$i = (x,y)\ ;\quad j = (x,y) \quad (15)$$

$$N_{xx} = \frac{E_0}{1-\nu^2}\left(\varepsilon_{x0} + \nu\varepsilon_{y0}\right) - \frac{E_1}{1-\nu^2}\left(\frac{\partial^2 w}{\partial x^2} + \nu\frac{\partial^2 w}{\partial y^2}\right) - \frac{\Phi_1}{1-\nu} \quad (16)$$

$$N_{yy} = \frac{E_0}{1-\nu^2}\left(\varepsilon_{y0} + \nu\varepsilon_{x0}\right) - \frac{E_1}{1-\nu^2}\left(\frac{\partial^2 w}{\partial y^2} + \nu\frac{\partial^2 w}{\partial x^2}\right) - \frac{\Phi_1}{1-\nu} \quad (17)$$

$$N_{xy} = \frac{E_1}{2(1+\nu\ )}\gamma_{xy0} - \frac{E_2}{(1+\nu\ )}\frac{\partial^2 w}{\partial x\,\partial y} \quad (18)$$

$$M_{xx} = \frac{E_1}{1-\nu^2}\left(\varepsilon_{x0} + \nu\varepsilon_{y0}\right) - \frac{E_2}{1-\nu^2}\left(\frac{\partial^2 w}{\partial x^2} + \nu\frac{\partial^2 w}{\partial y^2}\right) - \frac{\Phi_2}{1-\nu} \quad (19)$$

$$M_{yy} = \frac{E_1}{1-\nu^2}\left(\varepsilon_{y0} + \nu\varepsilon_{x0}\right) - \frac{E_2}{1-\nu^2}\left(\frac{\partial^2 w}{\partial y^2} + \nu\frac{\partial^2 w}{\partial x^2}\right) - \frac{\Phi_2}{1-\nu} \quad (20)$$

$$M_{xy} = \frac{E_2}{2(1+\nu\ )}\gamma_{xy0} - \frac{E_3}{(1+\nu\ )}\frac{\partial^2 w}{\partial x\,\partial y} \quad (21)$$

where E_i, ϕ_1, and ϕ_2 are given by the following equations:

$$E_i = \int_{-\frac{h}{2}}^{\frac{h}{2}} E(z)z^i dz\ ;\ \ i = (0;1;2;3)$$

$$\Phi_1 = \int_{-\frac{h}{2}}^{\frac{h}{2}} E(z)\alpha(z)T(z)dz$$

and

$$\Phi_2 = \int_{-\frac{h}{2}}^{\frac{h}{2}} E(z)\alpha(z)T(z)\ z\ dz$$

Based on classical plate theory, the non-linear equilibrium equations of a perfect plate are given by:

$$\frac{\partial N_x}{\partial x} + \frac{\partial N_{xy}}{\partial y} = 0 \quad (22)$$

$$\frac{\partial N_y}{\partial y} + \frac{\partial N_{xy}}{\partial x} = 0 \quad (23)$$

$$\frac{\partial^2 M_x}{\partial x^2} + \frac{\partial^2 M_y}{\partial y^2} + 2\frac{\partial^2 M_{xy}}{\partial x \partial y} + N_x\frac{\partial^2 w}{\partial x^2} + N_y\frac{\partial^2 w}{\partial y^2} + 2N_{xy}\frac{\partial^2 w}{\partial x \partial y} = 0 \quad (24)$$

The last equations may be rewritten into one equation in term of w by Substituting Eqs. (16)-(21) into Eqs. (22)-(24).

$$D\nabla^4 w - \left(N_x\frac{\partial^2 w}{\partial x^2} + N_y\frac{\partial^2 w}{\partial y^2} + 2N_{xy}\frac{\partial^2 w}{\partial x \partial y}\right) = 0 \quad (25)$$

Where D is given by:

$$D = \frac{E_2E_0 - {E_1}^2}{(1-\nu^2)E_0} \quad (25\text{ bis})$$

Note that for a uniform temperature variation, the derivatives of thermal force $\Phi_1$and moment Φ_2 with respect to x and y are zero, and consequently are omitted in the governing equations.

2.2.3 Compatibility Equation

To satisfy the first two equations of motion (Eqs. (22) and (23)), the Airy stress function f(x, y) will be utilized and which allows the in-plane stress resultants to be expressed by letting [5], [8], [15]:

$$N_{xx} = \frac{\partial^2 f(x,y)}{\partial y^2} \quad (26)$$

$$N_{yy} = \frac{\partial^2 f(x,y)}{\partial x^2} \quad (27)$$

$$N_{xy} = -\frac{\partial^2 f(x,y)}{\partial x \partial y} \quad (28)$$

For an imperfect FGM plate, Eq. (25) can be rewritten as:

$$D\nabla^4 w - \left[\frac{\partial^2 f}{\partial y^2}\left(\frac{\partial^2 w}{\partial x^2} + \frac{\partial^2 w^*}{\partial x^2}\right) + \frac{\partial^2 f}{\partial x^2}\left(\frac{\partial^2 w}{\partial y^2} + \frac{\partial^2 w^*}{\partial y^2}\right) - 2\frac{\partial^2 f}{\partial x \partial y}\left(\frac{\partial^2 w}{\partial x \partial y} + \frac{\partial^2 w^*}{\partial x \partial y}\right)\right] = 0 \quad (29)$$

where $w^*(x, y)$ represents a known small initial imperfection of the plate.

Note that the term $\nabla^4 w$ is unchanged, because it is obtained from the expression of bending moment M_{ij} and these internal moments don't rely on the value of the curvature but only on the amount of change of the curvature [6].

This gives one governing equation with two unknowns, w and f. To solve the problem, one more equation is needed in terms of the same unknowns. For this reason, the compatibility equation will be necessary and it's given by:

$$\frac{\partial^2 \varepsilon_{y0}}{\partial x^2} + \frac{\partial^2 \varepsilon_{x0}}{\partial y^2} - \frac{\partial^2 \gamma_{xy0}}{\partial x \partial y} = 0 \quad (30)$$

From Eqs. (26)-(28) and Eqs. (16)-(18), the compatibility equation can be rewriting as:

$$E_0\left[\left(\frac{\partial^2 w}{\partial x \partial y}\right)^2 - \frac{\partial^2 w}{\partial x^2}\frac{\partial^2 w}{\partial y^2} + 2\frac{\partial^2 w}{\partial x \partial y}\frac{\partial^2 w^*}{\partial x \partial y} - \frac{\partial^2 w}{\partial x^2}\frac{\partial^2 w^*}{\partial y^2} - \frac{\partial^2 w}{\partial y^2}\frac{\partial^2 w^*}{\partial x^2}\right] - \left[\frac{\partial^4 f}{\partial x^4} + 2\frac{\partial^4 f}{\partial x^2 \partial y^2} + \frac{\partial^4 f}{\partial y^4}\right] = 0 \quad (31)$$

Eqs. (29) and (31) are the general governing equations of thermal buckling of imperfect FG plate, which will be used in the next sections.

2.3 Boundary conditions and solution of the problem

To obtain the thermal load, the pre-buckling thermal stresses should be found. Consider that the FG plate is simply supported with immovable edges, the boundary conditions are:

$$w = u = M_x = 0\ ,\ N_x = N_{x0} \text{ on } x = 0, a \quad (32)$$

$$w = v = M_y = 0\ ,\ N_y = N_{y0} \text{ on } y = 0, b \quad (33)$$

where N_{x0} and N_{y0} are pre-buckling force resultants in directions x and y, respectively. With considering the boundary conditions, the approximate solutions are assumed [8,15]:

$$w = W\sin(\lambda x)\sin(\beta y) \quad (34)$$

$$w^* = \mu h\sin(\lambda x)\sin(\beta y) \quad (35)$$

$$\lambda = \frac{n\pi}{a}\ ;\ \beta = \frac{m\pi}{b} \text{ and } m, n = 1; 2; 3 \ldots, \quad (36)$$

$$f = f1\cos(2\lambda x) + f2\cos(2\beta y) + f3\sin(2\lambda x)\sin(2\beta y) + f4\cos(2\lambda x)\cos(2\beta y) + \frac{1}{2}N_{x0}x^2 + \frac{1}{2}N_{y0}y^2 \quad (37)$$

Where n and m denote half waves numbers in x and y directions, respectively. Also f1, f2, f3 and f4 are determined by substituting Eqs. (34)-(37) into Eq. (31):

$$f1 = E_0\frac{\beta^2}{32\lambda^2}W[W + 2\mu h] \quad (38)$$

$$f2 = E_0\frac{\lambda^2}{32\beta^2}W[W + 2\mu h] \quad (39)$$

$$f3 = f4 = 0 \quad (40)$$

Substituting Eqs. (34)-(37) into the stability equation; Eq. (29) and applying the Galerkin method [14–18] for the resulting equation, on can obtain:

$$D(\lambda^2 + \beta^2)W + \left[2\lambda^2\beta^2(f1 + f2) + \lambda^2 N_{x0} + \beta^2 N_{y0}\right](W + \mu h) = 0 \quad (41)$$

To determine the compressive stresses making all edges immovable: u=0 (on x=0, a) and v=0 (on y=0, b), the following condition must be verified [9,18]:

$$\iint_0^{b\,a}\frac{\partial u}{\partial x}\,dx\,dy = 0 \quad (42)$$

$$\iint_0^{a\,b}\frac{\partial v}{\partial y}\,dy\,dx = 0 \quad (43)$$

The expressions of $\frac{\partial u}{\partial x}$ and $\frac{\partial v}{\partial y}$ can be obtained by combining Eqs. (9)-(11), (15)-(18), (26)-(28) and (34)-(37). The imperfections are also accounted. Then, the expressions of compressive stresses are given by:

$$N_{x0} = \frac{E_1}{8(1-\nu^2)}(\lambda^2 + \nu\beta^2)(W + 2\mu h)W + \frac{4E_2}{ab(1-\nu^2)}\left(\frac{\lambda^2+\nu\beta^2}{\lambda\beta}\right)W - \frac{\Phi_1}{1-\nu} \quad (44)$$

$$N_{y0} = \frac{E_1}{8(1-\nu^2)}(\beta^2 + \nu\lambda^2)(W + 2\mu h)W + \frac{4E_2}{ab(1-\nu^2)}\left(\frac{\beta^2+\nu\lambda^2}{\lambda\beta}\right)W - \frac{\Phi_1}{1-\nu} \quad (45)$$

Introducing the above Eqs. (44) and (45) into Eq. (41), we obtain the expression of the thermal load:

$$\Phi_1 = \int_{-\frac{h}{2}}^{\frac{h}{2}} E(z)\alpha(z)\Delta T(z)dz = \int_{-\frac{h}{2}}^{\frac{h}{2}-h_c} E(z)\alpha(z)\Delta T(z)dz + \int_{\frac{h}{2}-h_c}^{\frac{h}{2}} E(z)\alpha(z)\Delta T(z)dz = \frac{hpi^2\,\bar{D}\left(n^2\left(\frac{b}{a}\right)^2+m^2\right)(1-\nu)}{\left(\frac{b}{h}\right)^2}\frac{W_h}{W_h+\mu} + \overline{E_1}\frac{h\,pi^2\left[(3-\nu^2)\left(n^4\left(\frac{b}{a}\right)^4+m^4\right)+4\nu\left(\frac{b}{a}\right)^2n^2m^2\right]}{16(1+\nu)\left(\frac{b}{h}\right)^2\left(n^2\left(\frac{b}{a}\right)^2+m^2\right)}W_h(W_h + 2\mu) + 4\overline{E_2}\frac{h\left(n^4\left(\frac{b}{a}\right)^4+m^4+2\nu n^2m^2\left(\frac{b}{a}\right)^2\right)}{mn\left(\frac{b}{h}\right)^2(1+\nu)\left(n^2\left(\frac{b}{a}\right)^2+m^2\right)}W_h \quad (46)$$

where:

$$W_h = \frac{W}{h} \;;\; \overline{E_1} = \frac{E_1}{h} \;;\; \overline{E_2} = \frac{E_2}{h^2} \;and\; \overline{D} = \frac{D}{h^2} \quad (47)$$

The final expression of the critical temperature of buckling depends in particular of the temperature distribution form and the plate initial temperature. In fact, the temperature is assumed to vary only through the thickness direction and is uniformly raised from the initial temperature $T_i = T_m$ to a final temperature T_f in which the plate buckles. Therefore, the temperature change is:

$$\Delta T(z) = T_f - T_i = T_f - T_m \quad (48)$$

In the next subsection, two types of temperature distribution will be considered.

2.4 Power law Temperature form

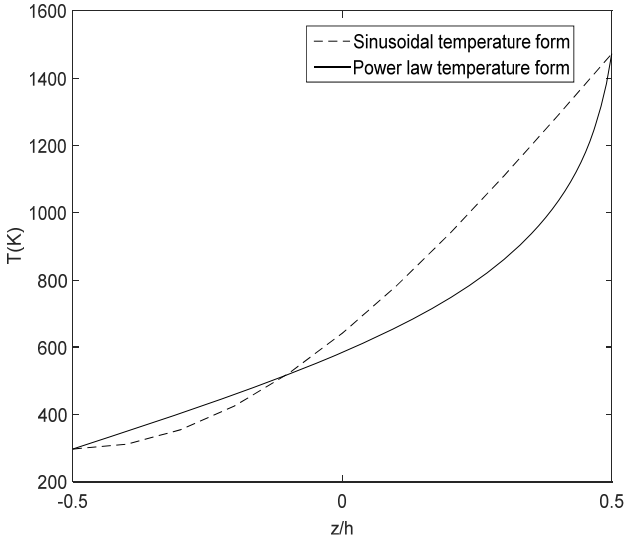

Fig. 2. Sinusoidal and power law temperature changes across the thickness for coated FG plate.

Assume a temperature variation through the thickness direction as (see Fig. 2):

$$T(z) = T_m + \Delta T\left(\frac{z}{h}+\frac{1}{2}\right)\frac{\sum_{i=0}^{inf}(-1)^i\frac{\left(\frac{z}{h}+\frac{1}{2}\right)^{ik}\left(\frac{K_{cm}}{K_m}\right)^i}{ik+1}}{\sum_{i=0}^{inf}(-1)^i\frac{\left(\frac{K_{cm}}{K_m}\right)^i}{ik+1}} \quad (49)$$

where:

$$\Delta T = T_c - T_m = T\left(\frac{h}{2}\right) - T\left(-\frac{h}{2}\right) \quad (50)$$

When the expression of temperature Eq. (49) is substituted into Eq. (46), the closed expression of the critical buckling temperature (ΔT_{cp}) of the coated FGM plate is obtained:

$$\Delta T_{cp} = \left[\begin{array}{c} \frac{pi^2\,\bar{D}\left(n^2\left(\frac{b}{a}\right)^2+m^2\right)(1-\nu)}{\left(\frac{b}{h}\right)^2}\frac{W_h}{W_h+\mu} + \\ \overline{E_1}\frac{pi^2\left[(3-\nu^2)\left(n^4\left(\frac{b}{a}\right)^4+m^4\right)+4\nu\left(\frac{b}{a}\right)^2n^2m^2\right]}{16(1+\nu)\left(\frac{b}{h}\right)^2\left(n^2\left(\frac{b}{a}\right)^2+m^2\right)} \\ W_h(W_h+2\mu) + \\ 4\overline{E_2}\frac{\left(n^4\left(\frac{b}{a}\right)^4+m^4+2\nu n^2m^2\left(\frac{b}{a}\right)^2\right)}{mn\left(\frac{b}{h}\right)^2(1+\nu)\left(n^2\left(\frac{b}{a}\right)^2+m^2\right)}W_h \end{array}\right] * \frac{hS}{(h-h_c)(Q+R)} \quad (51)$$

where:

$$Q = \sum_{i=0}^{5}\frac{\left(\frac{h-h_c}{h}\right)^{ik+1}\left(-\frac{K_{cm}}{K_m}\right)^i}{ik+1} * \left[\begin{array}{c} \frac{\alpha_m E_m}{ik+2}\left(\frac{h-h_c}{h}\right)^{ik+1} + \\ \frac{\alpha_{cm}E_m+\alpha_m E_{cm}}{(i+1)k+2}\left(\frac{h-h_c}{h}\right)^{(i+1)k+2} + \\ \frac{\alpha_{cm}E_{cm}}{(i+2)k+2}\left(\frac{h-h_c}{h}\right)^{(i+2)k+2} \end{array}\right] \quad (52)$$

$$R = \alpha_c E_c \sum_{i=0}^{5} \frac{\left(\frac{h-h_c}{h}\right)^{ik+1}\left(-\frac{K_{cm}}{K_m}\right)^{i}}{(ik+1)(ik+2)}\left[1-\left(\frac{h-h_c}{h}\right)^{ik+2}\right] \quad (53)$$

and

$$S = \sum_{i=0}^{5}(-1)^i \frac{\left(\frac{K_{cm}}{K_m}\right)^{i}}{ik+1} \quad (54)$$

2.5 Sinusoidal Temperature form

Assume a temperature variation through the thickness direction as (see Fig. 2) [10]:

$$T(z) = T_m + (T_c - T_m)\left[1-\cos\left(\frac{\pi z}{2h}+\frac{\pi}{4}\right)\right] \quad (55)$$

Similar to the preceding case, the critical buckling temperature (ΔT_{cs}) is obtained by substituting Eq. (55) into Eq. (46):

$$\Delta T_{cs} = \left[\begin{array}{c} \frac{pi^2\,\bar{D}\left(n^2\left(\frac{b}{a}\right)^2+m^2\right)(1-\nu)}{\left(\frac{b}{h}\right)^2}\frac{W_h}{W_h+\mu}+ \\ \overline{E_1}\frac{pi^2\left[(3-\nu^2)\left(n^4\left(\frac{b}{a}\right)^4+m^4\right)+4\nu\left(\frac{b}{a}\right)^2n^2m^2\right]}{16(1+\nu)\left(\frac{b}{h}\right)^2\left(n^2\left(\frac{b}{a}\right)^2+m^2\right)} \\ W_h(W_h+2\mu)+ \\ 4\overline{E_2}\frac{\left(n^4\left(\frac{b}{a}\right)^4+m^4+2\nu n^2m^2\left(\frac{b}{a}\right)^2\right)}{mn\left(\frac{b}{h}\right)^2(1+\nu)\left(n^2\left(\frac{b}{a}\right)^2+m^2\right)}W_h \end{array}\right]\frac{hF}{h-h_c} \quad (56)$$

where:

$$F = \left(E_m\alpha_m\left(\frac{h-h_c}{h}\right)+\frac{(E_m\alpha_{cm}+E_{cm}\alpha_m)}{k+1}\left(\frac{h-h_c}{h}\right)^{k+1}+\frac{E_{cm}\alpha_{cm}}{2k+1}\left(\frac{h-h_c}{h}\right)^{2k+1}\right)+E_c\alpha_c\left(\frac{h_c}{h}-I_{00}\right)-(E_m\alpha_m I_0+(E_{cm}\alpha_m+E_m\alpha_{cm})I_1+E_{cm}\alpha_{cm}I_2) \quad (57)$$

$$I_{00} = \int_{1-\frac{h_c}{h}}^{1}\cos\left(\pi\left(\frac{h-h_c}{2h}\right)z\right)dz \quad (58)$$

and

$$I_i = \int_0^{1-\frac{h_c}{h}}\cos\left(\pi\left(\frac{h-h_c}{2h}\right)z\right)z^{ik}dz\ ;\quad i=(0;1;2) \quad (59)$$

3 Results and discussion

1.

3.1 Verification

To further illustrate the accuracy of the results obtained, a comparison study is carried out for critical temperature buckling with the given results in the literature. The obtained results are compared with those predicted by [9]. As the $h_c \to 0$ from Eq. (51), the critical buckling non-uniform temperature rise (Power law form) of uncoated FGM plate is obtained. The plate is made from a mixture of metal (Aluminum) and ceramic (Alumina), and the material properties are taken to be:

$$E_m = 70\ GPa\ ,\quad \alpha_m = 23.10^{-6\circ}C^{-1}\ ,\quad K_m = 204\ \mathrm{W/mK}$$

$$E_c = 380\ GPa\ ,\quad \alpha_c = 7{,}4.10^{-6\circ}C^{-1}\ ,\quad K_c = 10{,}4\ \mathrm{W/m\,K}\ \text{and}\ \nu_m = \nu_c = 0.3$$

The data were taken from study [9,18,19]. The same properties are used in the rest of this work.

Fig. 3 represents a comparison of the obtained results with those predicted by [9].This figure clearly indicates that the results are in good agreement.

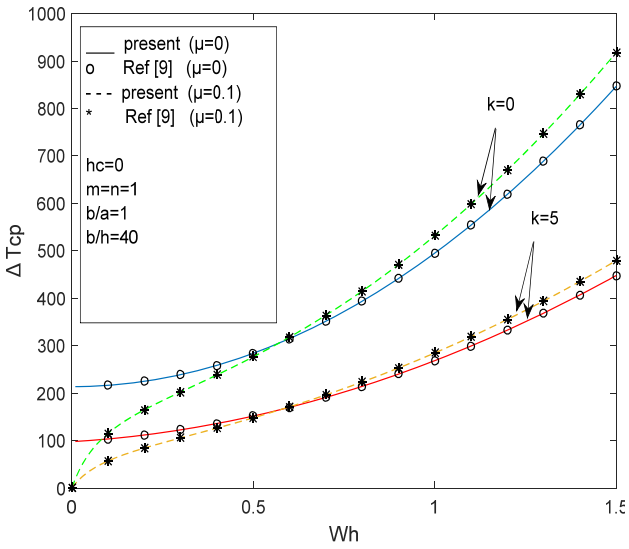

Fig. 3. Comparison of temperature-central deflection curves for perfect and imperfect FGM plates without coating.

In the following section, we will discuss the effect of the different parameters and the thickness of coating on the thermal buckling behavior of a FGM plate, subjected to two types of temperature rise (power law and sinusoidal).

3.2 Effect of coating thickness

Fig. 4 represents the effect of coating thickness on the critical buckling temperature for perfect and imperfect FG plate. Four values of h_c are considered h_c= (0; h/5; h/4; h/3). Fig. 4a concerns the plate subjected to the power law temperature form, and the Fig. 4b represents the sinusoidal temperature form. For the both cases, the critical buckling temperature increases by increasing ceramic coating thickness $h_c$and the difference becomes larger by increasing the deflection. In these figures, it is seen that the increase of the coating thickness for the case of sinusoidal temperature rise has a large stability effect on the plate than for the case of power law temperature rise.

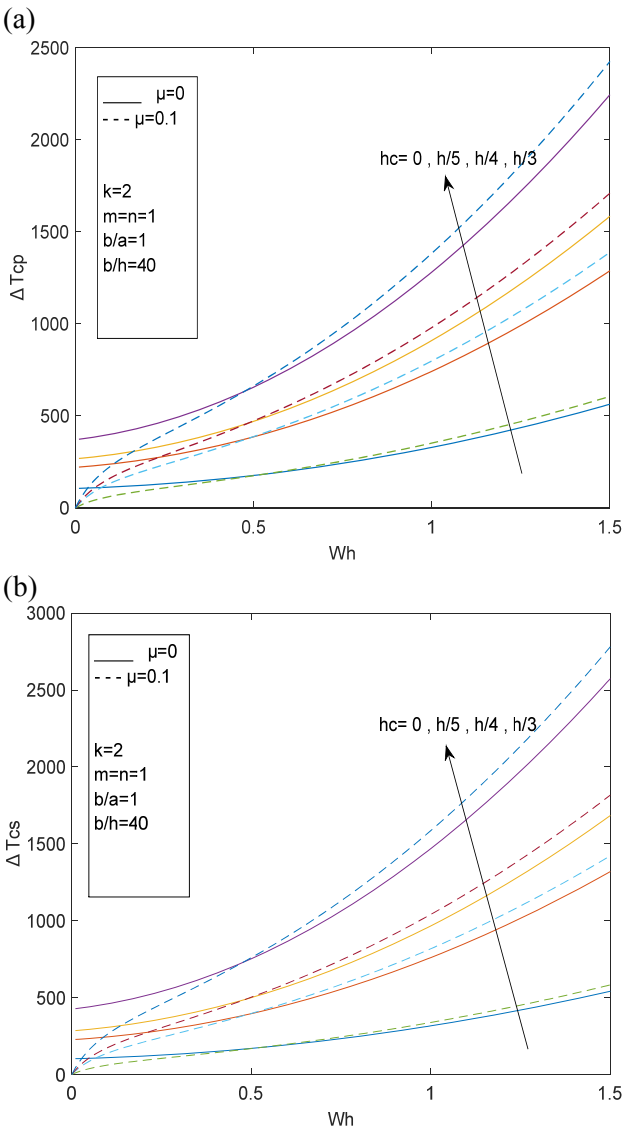

Fig. 4. Effect of coating thickness on the critical buckling temperature change: (**a)** power law temperature rise, (**b)** sinusoidal temperature rise.

3.3 Effect of imperfection size

Fig.5 represents the effect of imperfection size μ on the critical buckling temperature. Figs.5a and 5b concern the coated FGM plates subjected to the power law and sinusoidal temperature forms respectively. For the both cases, as the dimensionless deflection is small, the critical buckling temperature decreases by increasing imperfection size. In other words, the plate loses the buckling resistance. However, an opposite response is noticed when the deflection becomes large enough. Besides, the increase of imperfection size for the case of sinusoidal temperature rise has a large stability effect on the plate than for the case of power law temperature rise.

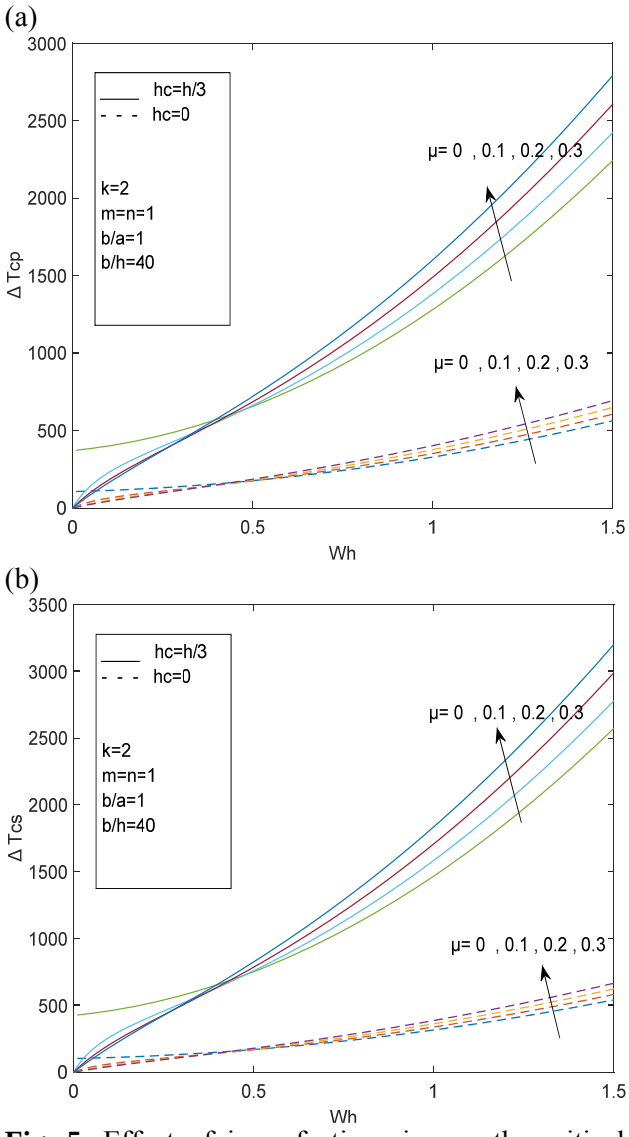

Fig. 5. Effect of imperfection size on the critical buckling temperature change: (**a)** power law temperature rise, (**b)** sinusoidal temperature rise.

3.4 Effect of power law index

When the coated functionally graded plate is subjected to the power law temperature form (see Fig. 6), the temperature-deflection curves reveal the existence of a critical power law index range corresponding to a high critical buckling temperature.

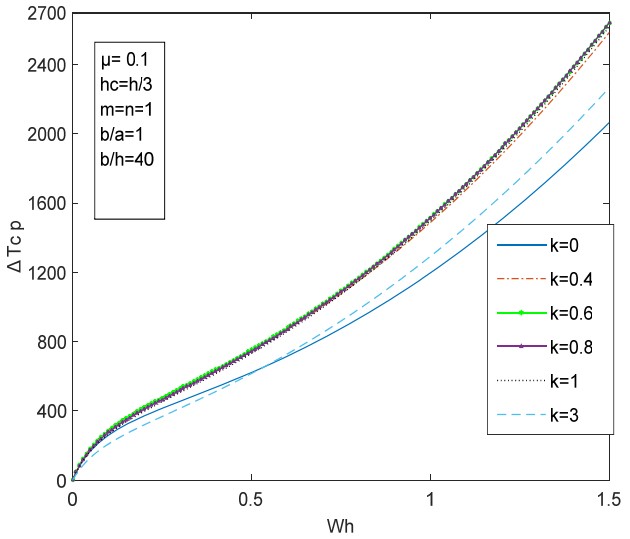

Fig. 6. Effect of power law index on the critical buckling temperature change for coated FGM plates, subjected to power law temperature rise.

As it can be seen in Fig. 7, for fixed values of the deflection, the optimum power law index increases slightly for 0 to 0.8 by increasing coating thickness between 0 and h/2. The optimum power law index stays at this interval even if the deflection is large. The obtained results are due to the fact that the nonlinearity of temperature distribution across the coating thickness depends of the power law index.

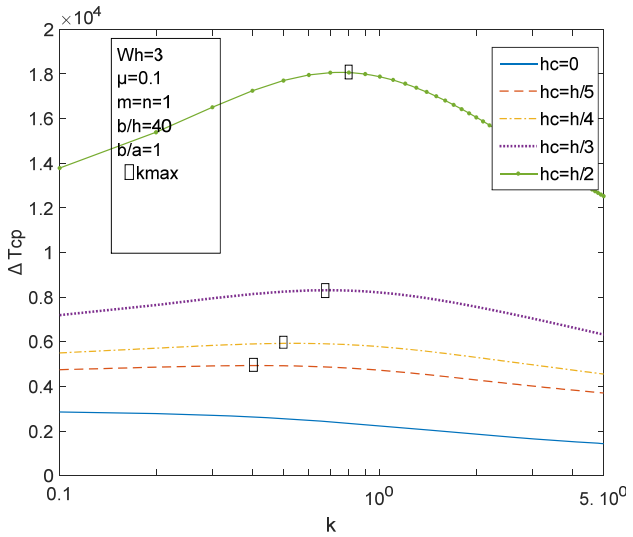

Fig. 7. Critical buckling temperature-power law index curves for imperfect FGM plates, subjected to a power law temperature rise.

As it relates to the sinusoidal temperature form, Figs.8 and 9 show another response. The critical buckling temperature decreases by increasing the power law index. In fact, the nonlinearity of the temperature form does not depend on the power law index. Thus, the influence of this index only reflects the direct effect of the material composition on the plate response. In other words, the plate becomes more stable when the volume fraction of the ceramic increases (k decreases).

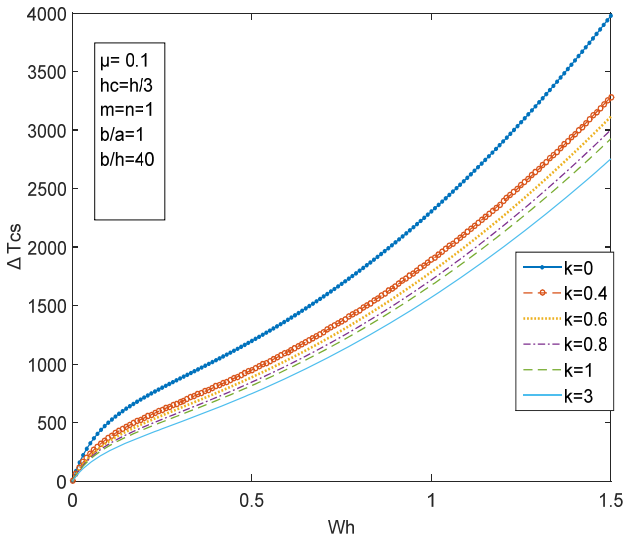

Fig. 8. Effect of power law index on the critical buckling temperature change coated FGM plates, subjected to a sinusoidal temperature rise.

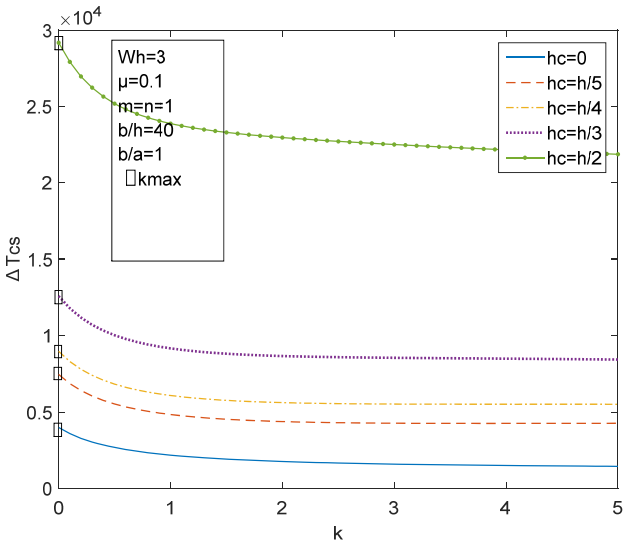

Fig. 9. Critical buckling temperature-power law index curves for imperfect FGM plates, subjected to a sinusoidal temperature rise.

3.5 Effect of geometrical parameters:

Figs. 10a and 10b represent the effects of the thickness ratio (b/h) on the critical temperature of buckling under the power law and sinusoidal temperature forms respectively. Figs. 11a and 11b represent the effect aspect ratio (b/a) on the critical temperature of buckling under the power law and sinusoidal temperature forms respectively.

The temperature-deflection curves are plotted with two values of thickness ratio b/h= (40; 60) and aspect ratio b/a= (1; 2).
From Figs. 10 and 11, the thermal buckling behaviors are the same for the two cases of temperature form. It can be seen that by increasing the thickness ratio (b/h) or the aspect ratio (b/a), the critical buckling temperature increases, because the plate stiffness increases by increasing these parameters. Also, it is observed that the increase of the thickness and aspect ratios for the case of sinusoidal temperature rise has a greater stability effect on the plate, than for the case of power law temperature rise.

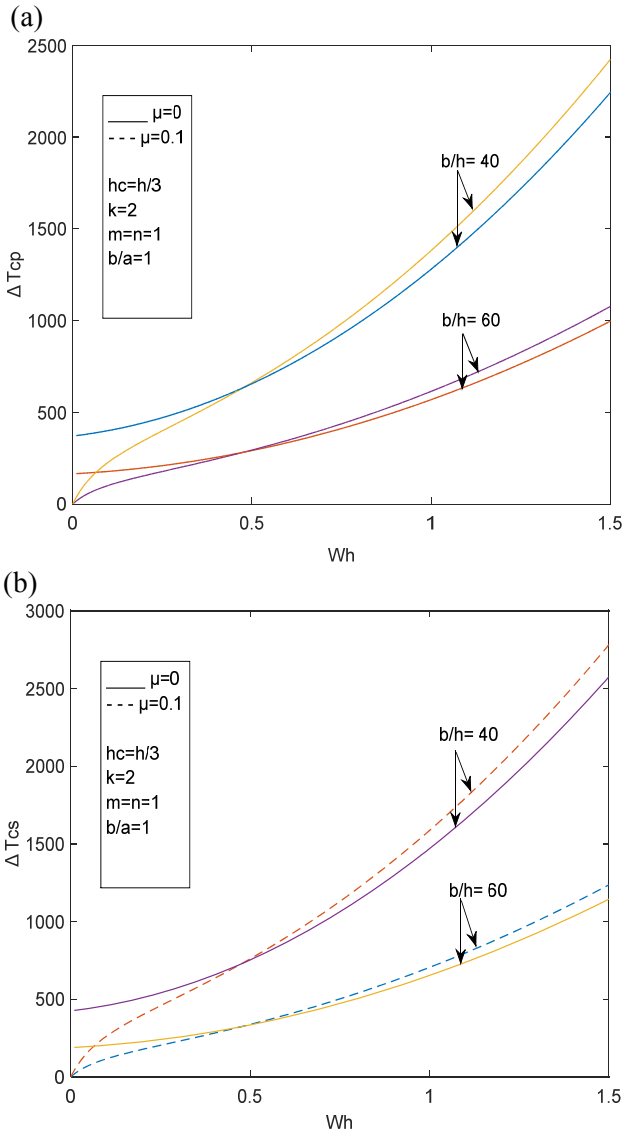

Fig. 10. Effect of thickness ratio on the critical buckling temperature change: (**a)** power law temperature rise. (**b)** sinusoidal temperature rise.

(a)

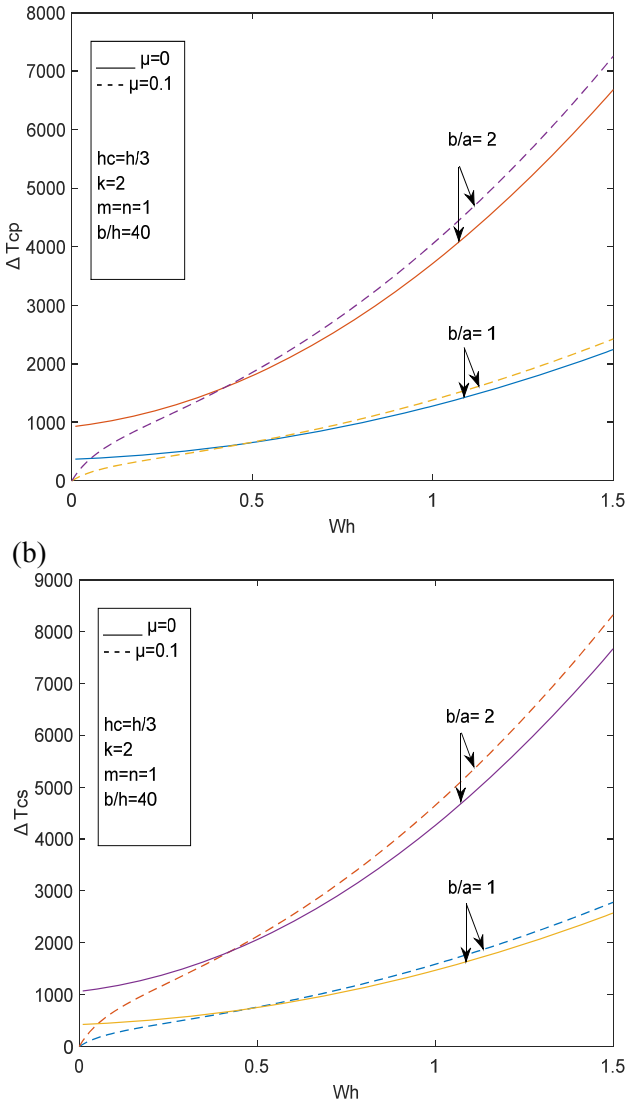

Fig. 11. Effect of aspect ratio on the critical buckling temperature change: (**a)** power law temperature rise. (**b)** sinusoidal temperature rise.

4 Conclusions:

In this study, an analytical solution has been presented for the buckling analysis of simply supported FGM plates with ceramic coating. Firstly, the plate's governing equations for the structural analysis were derived by CPT assumption, then, the closed expression of critical buckling temperature was obtained by applying Galerkin Method. Finally, influences played by different thermal fields, material composition and geometrical parameters were discussed in detail. It can be concluded that:
-The thermal post-buckling behaviors are different for the plates under sinusoidal and power law temperature rises.
-The critical temperatures calculated from power law temperature distribution are smaller than those from sinusoidal law.

-The increase of coating thickness plays an important role in the structure protection counter the failure.
-Increasing the size of imperfections for the case of large deflections makes the plate more stable.
-The stability was also improved by limiting the power law index between 0 and 0.8 in the case of power law temperature rise or by decreasing this index in the case of the sinusoidal temperature rise.
-The increase of thickness or aspect ratios increases the plate stiffness and gives more buckling resistance.
-The increase of the imperfection size, the aspect or the thickness ratios for the case of sinusoidal temperature rise has a greater stability effect on the plate, than for the case of power law temperature rise.

Acknowledgment: The authors would like to thank the Associate Editor for his support and assistance with the review of the paper.

References:

[1] Koizumi M, FGM activities in Japan, Compos PART B, Vol.8368, 1997, 1–4.
[2] Javaheri R, Thermal Buckling of Functionally Graded Plates,Vol.40, 2002.
[3] Kiani Y, Bagherizadeh E, Eslami MR, Thermal buckling of clamped thin rectangular FGM plates resting on Pasternak elastic foundation (Three approximate analytical solutions), Vol.593, 2011, 581–93. doi:10.1002/zamm.201000184.
[4] Lanhe W, Thermal buckling of a simply supported moderately thick rectangular FGM plate, Vol.64, 2004, 211–8. doi:10.1016/j.compstruct.2003.08.004.
[5] Samsam Shariat BA, Eslami MR, Effect of Initial Imperfections on Thermal Buckling of Functionally Graded Plates, J Therm Stress, 2005. doi:10.1080/014957390967884.
[6] Samsam Shariat BA, Eslami MR, Thermal buckling of imperfect functionally graded plates, Int J Solids Struct, 2006. doi:10.1016/j.ijsolstr.2005.04.005.
[7] Shariat BAS, Eslami MR, Buckling of thick functionally graded plates under mechanical and thermal loads, Compos Struct, Vol.78, 2007, 433–9. doi:10.1016/j.compstruct.2005.11.001.
[8] Yang J, Imperfection sensitivity of the post-buckling behavior of higher-order shear deformable functionally graded plates, Vol.43, 2006, 5247–66. doi:10.1016/j.ijsolstr.2005.06.061.
[9] Tung H Van, Duc ND, Nonlinear analysis of stability for functionally graded plates under mechanical and thermal loads, Compos Struct, Vol.92, 2010. doi:10.1016/j.compstruct.2009.10.015.
[10] Fazzolari FA, Natural frequencies and critical temperatures of functionally graded sandwich plates subjected to uniform and non-uniform temperature distributions, Compos Struct, Vol.121 2015. doi:10.1016/j.compstruct.2014.10.039.
[11] Reddy JN, Analysis of functionally graded plates, Vol.684, 2000, 663–84.
[12] Li SR, Zhang JH, Zhao YG, Nonlinear thermomechanical post-buckling of circular FGM plate with geometric imperfection, Thin-Walled Struct, Vol.45, 2007, 528–536. doi:10.1016/j.tws.2007.04.002.
[13] Zenkour AM, Sobhy M, Thermal buckling of various types of FGM sandwich plates, Compos Struct, Vol.93, 2010, 93–102. doi:10.1016/j.compstruct.2010.06.012.
[14] Shen HS, Thermal postbuckling behavior of shear deformable FGM plates with temperature-dependent properties, Int J Mech Sci, Vol.49, 2007, 466–478. doi:10.1016/j.ijmecsci.2006.09.011.
[15] Tung H Van, Thermal and thermomechanical postbuckling of FGM sandwich plates resting on elastic foundations with tangential edge constraints and temperature dependent properties, Compos Struct, Vol.131, 2015, 1028–1039. doi:10.1016/j.compstruct.2015.06.043.
[16] Van Tung H, Nonlinear axisymmetric response of FGM shallow spherical shells with tangential edge constraints and resting on elastic foundations, Compos Struct, 2016. doi:10.1016/j.compstruct.2016.04.032.
[17] Wang Z, Han Q, Nash DH, Liu P, Hu D, Investigation of imperfect effect on thermal buckling of cylindrical shell with FGM coating, Eur J Mech / A Solids, Vol.69, 2018, 221–30. doi:10.1016/j.euromechsol.2018.01.004.
[18] Sofiyev AH, Thermoelastic stability of freely supported functionally graded conical shells within the shear deformation theory, Compos Struct, Vol.152, 2016,74–84. doi:10.1016/j.compstruct.2016.05.027.
[19] So AH, Zerin Z, Kuruoglu N, Thermoelastic buckling of FGM conical shells under non-linear temperature rise in the framework of the shear deformation theory, Vol.108 , 2017, 279–90. doi:10.1016/j.compositesb.2016.09.102.
[20] Dag S, Thermal fracture analysis of orthotropic functionally graded materials using an equivalent domain integral approach, Vol.73, 2006, 2802–28. doi:10.1016/j.engfracmech.2006.04.015.

[21] JOHNS DJ, Thermal Stress Analyses, Therm Stress Anal, 1965, 21–32. doi:10.1016/B978-1-4832-1361-3.50008-7.

List of Symbols

h_c Ceramic coating thickness.
a, b Plate length and width.
h Plate thickness.
P Material property
V Volume fraction of the ceramic phase
k Power law index
$K(z), K_c, K_m$ Thermal conductivity at z coordinate, Ceramic and Metal.
(x, y, z) Cartesian coordinates.
$(\mathrm{U}, \mathrm{V}, \mathrm{W})$ Displacement components along the x, y and z directions respectively.
$(\mathrm{u}, \mathrm{v}, \mathrm{w})$ Displacement components of point on the mid-plane (z=0) along the x, y, z directions respectively.
w^* Initial geometrical imperfection.
$(\varepsilon_x, \varepsilon_y, \gamma_{xy})$ Normal and shear strains.
$(\varepsilon_{x0}, \varepsilon_{y0}, \gamma_{xy0})$ Normal and shear strains of point on the mid-plane (z=0).
$(\sigma_x, \sigma_y, \tau_{xy})$ Normal and shear stresses.
$(\sigma_{x0}, \sigma_{y0}, \tau_{xy0})$ Normal and shear stresses of point on the mid-plane (z=0).
$\mathrm{E}(z), E_c, E_m$ Young Modulus of the plate, Ceramic and Metal.
G Shear modulus.
$\alpha(z), \alpha_c, \alpha_m$ Thermal expansion coefficient at z coordinate, Ceramic and Metal.
$\nu(z), \nu_c, \nu_m$ Poisson ratioat z coordinate, Ceramic and Metal.
N_{ij} Normal and shearing force intensities.
M_{ij} Bending and twisting moment intensities.
$(\mathrm{N}_{x0}, \mathrm{N}_{y0})$ Pre-buckling force intensities in directions x and y.
Φ_1 Normal force due to the thermal effects.
Φ_2 Bending moment due to the thermal effects.
F Airy stress function.
μ Imperfection size.
m, n Half waves numbers in x and y directions
$\mathrm{T}(z), T_c, T_m$ Temperature at z coordinate, bottom and top faces.
$\Delta T_{cs}, \Delta T_{cp}$ Critical buckling temperature difference corresponding to Sinusoidal and power law temperature form.